A proteomic approach to the investigation of early events involved in vascular smooth muscle cell activation

Cell Tissue Res (2007) 328:185–195
DOI 10.1007/s00441-006-0357-3

REGULAR ARTICLE

A proteomic approach to the investigation of early events involved in vascular smooth muscle cell activation

Claudia Boccardi · Antonella Cecchettini · Anna Caselli · Guido Camici · Monica Evangelista · Alberto Mercatanti · Giuseppe Rainaldi · Lorenzo Citti

Received: 27 February 2006 / Accepted: 31 October 2006 / Published online: 10 January 2007

Abstract Vascular smooth muscle cells (VSMC) are mature cells that maintain great plasticity. This distinctive feature is the basis of the VSMC migration and proliferation involved in cardiovascular diseases. We have used a proteomic approach to the molecular changes that promote the switch of VSMC from having a quiescent to activated-proliferating phenotype. In particular, we have focused on modulations occurring during tyrosine-phosphorylation following cell activation by serum or single growth factors, such as insulin-like growth factor 1 or platelet-derived growth factor. A comparison of two-dimensional polyacrylamide gel profiles from quiescent or activated-proliferating VSMC has allowed us to recognize a number of differences in protein expression. Several differentially expressed proteins have been identified by mass spectrometry, and their time-course changes during tyrosine-phosphorylation have been documented from time zero till 48 h after stimulation. We have documented a general decrease of the tyrosine-phosphorylation level within the first few minutes after stimulation followed by a recovery that is quick and dramatic for some chaperones and redox enzymes but not so significant for enzymes of glucose metabolism. With regard to cytoskeleton components, no remarkable fluctuations have been detected at the earliest time points, except for those relative to α-actin, which displays an impressive decrease. A comparison of the early stages of cell stimulation after the administration of serum or single growth factors has brought to light important differences in the phosphorylation of chaperones, thereby suggesting their crucial role in VSMC activation.

Keywords Vascular smooth muscle cells · Growth factors · Proteomics · Phenotype · Chaperones · Pig

This work was partially supported by two FIRB 2001 project grants to Dr. G. Rainaldi and to Prof. G. Camici.

C. Boccardi · M. Evangelista · A. Mercatanti · G. Rainaldi · L. Citti
Laboratory of Molecular and Gene Therapy,
Clinical Physiology Institute CNR,
Pisa, Italy

C. Boccardi
Department of Internal Medicine, University of Pisa,
Pisa, Italy

A. Cecchettini
Department of Human Morphology and Applied Biology,
University of Pisa,
Pisa, Italy

A. Caselli · G. Camici
Department of Biochemical Sciences, University of Florence,
Florence, Italy

L. Citti (✉)
Clinical Physiology Institute CNR,
Via Moruzzi 1,
56124 Pisa, Italy
e-mail: lorenzo.citti@ifc.cnr.it

Introduction

Vascular smooth muscle cells (VSMC) are mature cells that maintain great plasticity and are capable of switching easily from a contractile state to an activated synthetic phenotype (Owens et al. 2004). Such plasticity is the basis of VSMC migration and proliferation involved in the formation of atheromas and/or hyperplasia of the neointima following stent implantation. In the arterial wall, VSMC lie behind the endothelium, which separates them from the blood flow. When the vessel is injured, serum comes into contact with VSMC, and growth factors, cytokines, and many other soluble components probably interact with the plasma membrane of the muscle cells, thereby activating complex

signaling cascades. Among the elements involved in cell activation, growth factors are the most extensively studied, as several of them contribute to the formation of atherosclerotic and restenotic lesions (for reviews, see Ross 1993; Cercek et al. 1991).

Our study focuses on the role of serum in SMC activation compared with that of single growth factors such as insulin-like growth factor 1 (IGF-1) and platelet-derived growth factor (PDGF-BB). PDGF and IGF are important regulators of VSMC death and proliferation (Kamide et al. 2000; Bayes-Genis et al. 2000; Hayashi et al. 2004). IGF-1 and PDGF-BB are known to act in synergy toward the induction of cellular proliferation (Clemmons 1985), probably through the up-regulation of IGF-receptor expression (Delafontaine et al. 1991; Rubini et al. 1994). Antisense oligonucleotides, which inhibit the expression of the IGF-receptor, reduce thrombin, angiotensin II, and PDGF-induced mitogenesis in VSMC (Delafontaine et al. 2004), indicating that IGF-receptor activation is a rate-limiting step in cell-cycle progression (Baserga and Rubin 1993).

PDGF-BB is known as the most potent chemoattractant and mitogen for VSMC (Heldin and Westermack 1990; Thyberg et al. 1990). During injury to blood vessels, PDGF triggers phenotypic modulation, which is mediated by changes in patterns of gene expression. Recently, a subset of genes has been defined that are up- or down-regulated in VSMC by PDGF (Kaplan-Albuquerque et al. 2005).

To date, studies have focused on the gene expression profile involved in VSMC phenotypic modulation and have produced some insight into the specific genes involved in this process and their regulation. However, none have succeeded in correlating either the genomic sequence or the transcriptional profile with protein activation. Because the importance of detaching functional proteins is becoming increasingly clearer, we have tried a proteomic approach to the study of VSMC activation. The most detailed map of VSMC proteins that is currently available is that of McGregor et al. (2001) who have studied the human saphenous vein. An extensive protein profile of human arterial VSMC has only recently been obtained (Dupont et al. 2005).

In this study, we have focused our attention on early stages of phenotypic modulation of VSMC following stimulation by serum and growth factors, with an attempt to identify some key elements of the complex activation network at the initiation of phenotypic remodeling. In order to gain further insights into the activation process, we have examined time-course changes in tyrosine-phosphorylation for 20 sequenced proteins.

In the early phases of the activation process, cells are engaged in rapid responses that cannot rely on the synthesis of new proteins but that probably depend upon previously existing and post-translationally modified molecules. Consequently, the molecules that are modulated in such a short time could represent good prognostic markers and/or useful pharmacological targets.

Materials and methods

Isolation of SMC and culture conditions

Coronaries were dissected from the myocardium of 3-month-old domestic crossbred pigs (*Sus scrofa domestica*). Medial VSMC were isolated by enzymatic digestion and cultured according to the method described by Christen et al. (1999). All experiments reported in this study were performed with VSMC from between the second and the sixth passages and, unless otherwise specified, from at least three different explants.

The investigation conforms to the Guide for the Care and Use of Laboratory Animals published by the US National Institutes of Health (NIH Publication no. 85–23, revised 1996).

Cell cycle

Cells were fixed in 70% ethanol for 2 h at −20°C and permeabilized with 0.25% Triton X-100 for 5 min at 4°C. Cell suspensions were then centrifuged, and the pellets were resuspended in 250 µl phosphate-buffered saline (PBS) containing 100 mg/ml propidium iodide (Roche), 0.1 mg/ml RNAse (Roche), and 0.5% IGEPAL CA 630 (Sigma). Cells were passed through a flow cytometer (FACScalibur, Becton Dickinson), and cell-cycle analysis was carried out by using Cell Quest analysis software (Becton Dickinson).

Chemotactic activity

Chemotaxis was assayed in Boyden chambers (Neuro Probe). The chemoattractant used was 10% FBS in HG DMEM, which was placed in the lower chamber. Bovine serum albumin (0.1% BSA; fraction V, Sigma) was used as a control under similar experimental conditions. Polyvinylpyrrolidone-free 8-µm-pore polycarbonate filters were coated with 5 mg/l porcine skin gelatin (Sigma) and placed between the upper and lower chambers. Cells, suspended in HG DMEM with 0.1% BSA, were placed in the upper chambers at a density of 2×10^5 cells/chamber. After 5 h of incubation at 37°C, filters were fixed in absolute ethanol for 30 s and stained with 2% toluidine blue (Sigma). Migrating cells were counted on the lower side of the filter. Fifteen fields for each filter were analyzed, and data were reported as the average number of cells per field.

Immunofluorescence analysis

Immunofluorescence analysis was carried out on cells grown on coverslips. The cells were fixed for 30 min at 4°C with 2% paraformaldehyde in PBS and incubated overnight with anti-SM-α-actin (1:200; Sigma, St Louis, USA) or anti-smoothelin (1:4; R4A, Chemicon) monoclonal antibodies. Incubation with the secondary antibody, viz., Alexa Fluor 568 goat anti-mouse IgG (H+L) (1:3,000; Molecular Probes), was performed at room temperature for 2 h. A few specimens were treated with rhodamine-labeled phalloidin (Molecular Probes) for 20 min (1 unit in 200 μl blocking solution per slide).

Two-dimensional gel electrophoresis, image acquisition, and data analysis

Cell extracts Pellets from 10^6 VSMC were suspended in 250 μl conventional ice-cold two-dimensional (2-D) lysis medium containing 8 M urea, 4% (w/v) CHAPS, 1% (w/v) dithiothreitole (DTT), and 1 mM sodium orthovanadate. Cells were gently vortexed and centrifuged at 13,000 rpm at 4°C for 45 min, and the supernatant was stored at −80°C until used. The protein concentration was determined by Bradford's procedure (Bio-Rad Protein Assay, Bio-Rad).

Protein separation by isoelectrofocusing (1st dimension) Separation by isoelectrofocusing (IEF) was carried out according to the method originally described in Görg et al. (1988) with pre-manufactured 18-cm-length strips displaying an immobilized non-linear pH gradient ranging from 3 to 10 (Amersham Biosciences, Uppsala, Sweden) run on a Ettan IPGphor system (Amersham Biosciences). For analytical runs, IPG strips were loaded and rehydrated at 16°C with 100 μg protein crude extracts in 350 μl lysis buffer and 0.2% (v/v) carrier ampholyte (IPG buffer or Pharmalyte 3–10) at 0 V for 1 h and at 30 V for an additional 8 h. Focusing was performed at 16°C under the following conditions: 200 V for 1 h, 300–3,500 V for 30 min, 3,500 V for 1 h, 3,500–8,000 V for 30 min, and 8,000 V until a total 80,000 Vh was attained. For preparative runs, strips were loaded and rehydrated according to the above conditions with 1,000 μg crude extracts in the 350 μl lysis buffer.

Protein separation by denaturating gradient polyacrylamide gel electrophoresis (2nd dimension) Strips from the above analytical or preparative 1st dimensional separation were equilibrated for 12 min at room temperature in a medium containing 6 M urea, 2% (w/v) SDS, 2% (w/v) DTT, 30% (w/v) glycerol, and 0.05 M TRIS-HCl buffer pH 6.8 and then for an additional 5 min in a medium containing 6 M urea, 2% (w/v) SDS, 2.5% (w/v) iodoacetamide, 30% glycerol, 0.05 M TRIS-HCl buffer, pH 6.8, and a trace of bromophenol blue. The gel strips were loaded onto the top of a 20 cm×20 cm×1.5 mm linear gradient polyacrylamide gels ranging from 9% to 16% polyacrylamide. Runs were carried out at 9°C under constant voltage at 120 V until the dye front had reached the bottom of gel.

Gel staining and image analysis For analytical runs, gels were stained in ammoniacal silver nitrate according to the method described in Hochstrasser et al. (1988). Gels in preparative runs were stained in a highly sensitive colloidal Coomassie G-250 blue dye according to the "Blue Silver" protocol as described in Candiano et al. (2004). Stained gels were scanned by using an Epson Expression 1680 Pro Scanner (Seiko Epson, Japan), and digital images were recorded and stored in appropriate formats. The analysis of digital images was carried out with Image Master computer software (GeneBio, Geneva, Switzerland). Values for the isoelectric point (Ip) and mass (Da) of each spot were calculated on the basis of separate co-migration runs performed with human serum introduced as an internal standard.

Immunodetection of Tyr-phosphoproteins Crude protein extracts (120 μg) were separated by 2D gel electrophoresis (2D-PAGE) and transferred onto nitrocellulose membranes (Hybond-C, Amersham Life Science). Membranes were checked for protein resolution with Ponceau red staining and incubated overnight at 4°C with a mouse anti-phosphotyrosine monoclonal antibody (IgG_{2b}; Santa Cruz Biotechnology) diluted 1:1,000 in 3% BSA, 0.1% Tween-20 in PBS and then with the secondary antibody, viz., a sheep anti-mouse IgG (Santa Cruz Biotechnology), diluted 1:3,000, for 1 h at room temperature. Chemiluminescence was detected by using an ECLTM Detection Kit (Amersham Biosciences).

Protein identification by mass spectrometry

Electrophoretic spots, visualized by colloidal Coomassie G-250 staining, were excised manually, destained according to the method described in Shevchenko et al. (1996), and dehydrated. Successively, a trypsin solution was added, and in-gel protein digestion was performed by overnight incubation at 37°C. Digested peptides (0.75 μl/spot) were mixed with 0.75 μl matrix solution, viz., a saturated solution of cyclohexane carboxylic acid in 50% (v/v) acetonitrile and 0.1% (v/v) trifluoroacetic acid, spotted onto a MALDI plate and then allowed to dry. Peptide mass fingerprintings were acquired by using a OmniFLEX MALDI-TOF mass spectrometer (Bruker Daltonics Corporation, Billerica, Mass., USA). Peptide mass fingerprinting

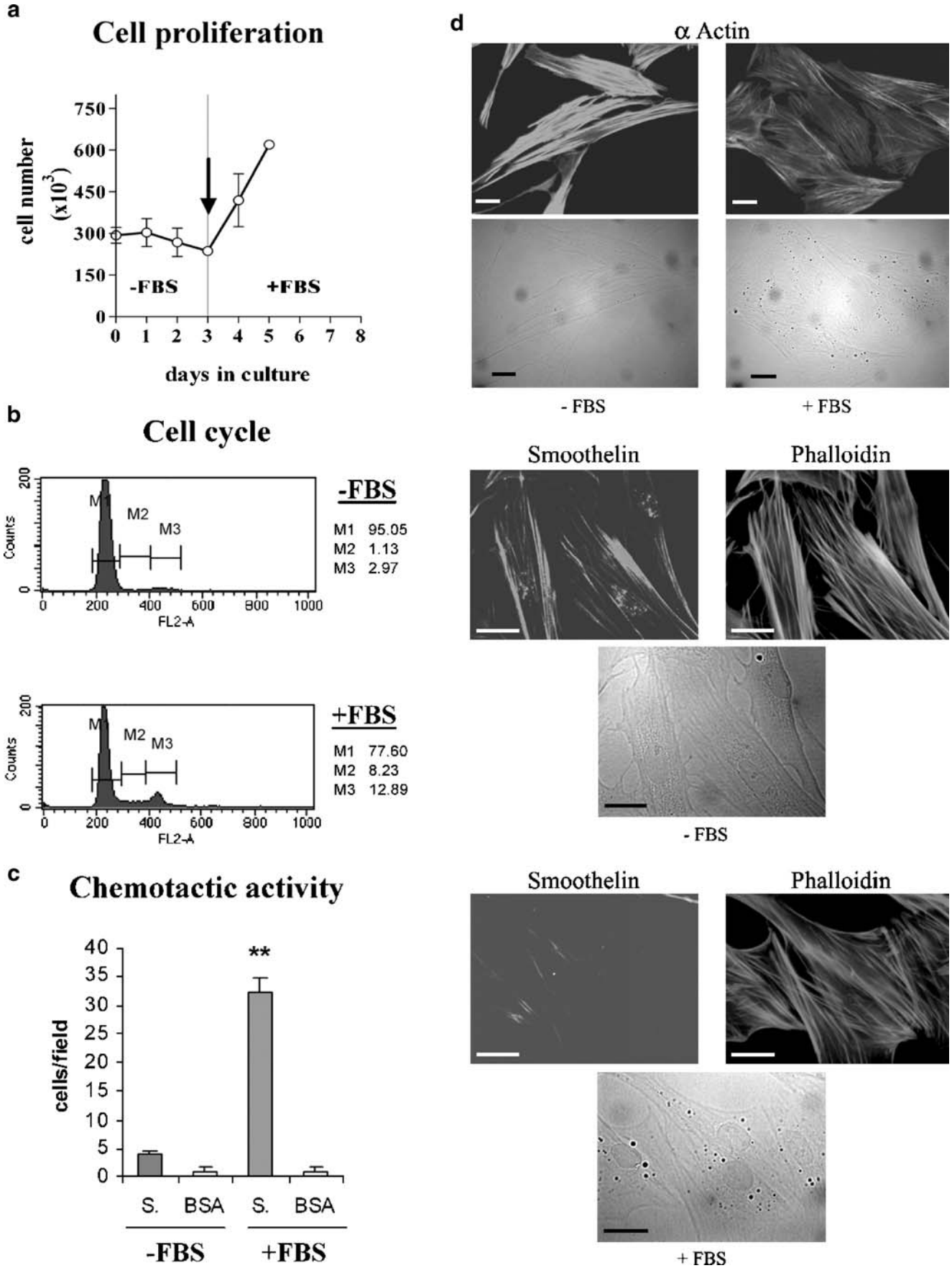
a
Cell proliferation
cell number (x10^3)
750
600
450
300
150
0
-FBS
+FBS
0 1 2 3 4 5 6 7 8
days in culture
b
Cell cycle
Counts
M1
M2
M3
-FBS
M1 95.05
M2 1.13
M3 2.97
FL2-A
+FBS
M1 77.60
M2 8.23
M3 12.89
c
Chemotactic activity
cells/field
**
S. BSA S. BSA
-FBS +FBS
d
α Actin
- FBS
+ FBS
Smoothelin
Phalloidin
- FBS
+ FBS

◀ **Fig. 1** **a** Cell proliferation. VSMC were maintained for 3 days in serum free medium (*-FBS*) in order to consolidate the quiescent phenotype. After this time (*arrow*), a complete medium, supplemented with a 10% fetal bovine serum, was added (*+FBS*), and the cells were cultured for 2 additional days. Cells were counted every day. Each point represents the mean±SD of three independent experiments. **b** Cell cycle. The same samples as those in **a** (*−FBS*, *+FBS*) were subjected to flow cytometric analysis. The *M1*, *M2*, and *M3* gates correspond to the G_0/G_1, S, and G_2/M phases of cell cycle, respectively. The mean±SD of three independent experiments is reported. **c** Chemotactic activity. VSMC were allowed to migrate through gelatin-coated filters in response to 10% FBS (*S.*) or 0.1% BSA (*BSA*) as chemoattractors. Data were compared by using the unpaired *t*-test. $^{**}P<0.01$. Each *bar* shows the mean ±SD of three independent experiments. **d** Cytoskeleton proteins. VSMC were analyzed by immunofluorescence microscopy in the absence of serum (*−FBS*) or in serum-supplemented medium for 2 days (*+FBS*). Exposure to rhodamine-labeled phalloidin demonstrated the presence of actin filaments. Smooth muscle markers were revealed by immunolabeling for α-actin and smoothelin. The corresponding phase-contrast images are shown *bottom*. Results are representative of three independent experiments. *Bar* 40 μm

searches were carried out by using software available online: ProFound, (http://www.129.85.19.192/profound_bin/WebProFound.exe); PeptIdent, (http://www.expasy.org); MASCOT (Matrix Science, London, UK; http://www.matrixscience.com).

Results

VSMC, isolated from porcine coronaries and grown under standard conditions in complete medium, displayed a synthetic phenotype endowed with migrating properties and proliferating activities. When serum was completely withdrawn from culture medium (minus fetal bovine serum, −FBS), cells rapidly switched to a quiescent-contractile phenotype. Under these conditions, VSMC stopped proliferating (Fig. 1a), blocking their cell cycle at the G1/G0 stage (Fig. 1b) without becoming apoptotic (data not shown), and lost all chemotactic activity (Fig. 1c). They acquired an elongated spindle-shaped morphology and expressed cytoskeleton proteins specific for the contractile phenotype, such as α-actin and smoothelin (Fig. 1d). The addition of 10% FBS (+FBS) to medium switched cultures back to a proliferating (Fig. 1a,b) and migrating (Fig. 1c) type, supporting a round-shaped flat morphology, a decrease in α-actin expression, and a more consistent reduction in smoothelin (Fig. 1d).

For further insights into such phenotypic changes, 2D-PAGE was employed. VSMC were cultured for 2 days in the absence of serum to induce the quiescent-contractile phenotype. Cultures were then split into two fractions: the first was immediately collected, whereas the second was left for 2 additional days in complete medium to produce the activated cells. Both recovered samples were processed for 2D-PAGE analysis. Master gels (mean of four replicas) from quiescent-contractile and activated VSMC (shown in Fig. 2a,b, respectively) were analyzed to identify the spots differentially expressed. Of the spots, 105 were up-regulated, and 154 were down-regulated in activated cells compared with those observed in the quiescent-contractile state.

Some of the differentially expressed spots were localized in a Coomassie-blue-stained preparative gel. These spots were excised, digested in-gel by trypsin, and sequenced by mass spectrometry. Sequenced proteins were subdivided into three principal categories: (1) enzymes involved in redox regulation and chaperones, viz., peroxiredoxin 3, peroxiredoxin 4, protein disulfide isomerase (PDI), reticulocalbin, Hsp60 and Hsp27; (2) cytoskeleton elements, viz., tropomyosin α4 and α1 chain tropomyosin, α- and γ-actins, vimentin, cytokeratin 10; (3) glucose metabolism enzymes, viz., α-enolase, ATP synthase, pyruvate kinase, and pyruvate dehydrogenase. Four other proteins, viz., hnRNP H, phohibitin, casein precursor and α−(B)crystallin, were also identified but could not be restricted into a specific class, even though they are all known to have

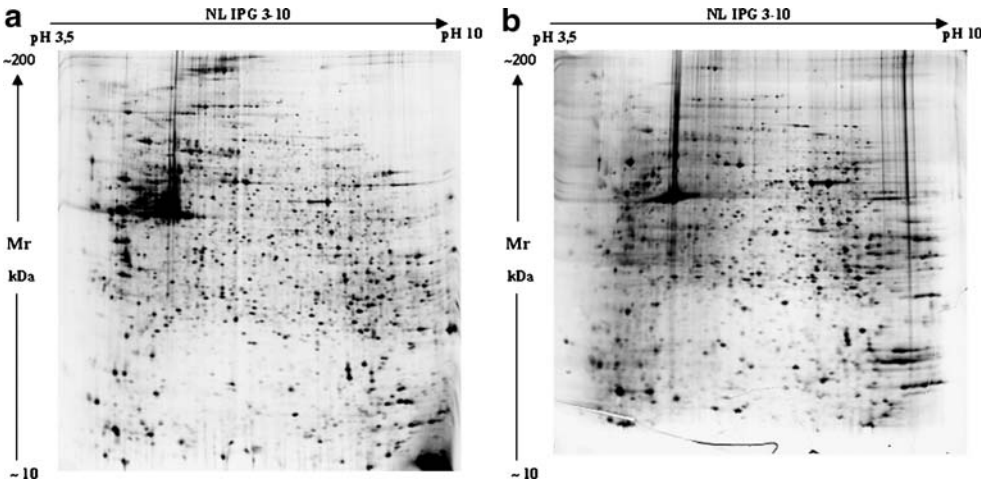

Fig. 2 Two-dimensional polyacrylamide gel electrophoresis (2D-PAGE). Master gels as the mean of four independently run replicates of protein extracts from quiescent-contractile (**a**) and serum-activated (**b**) VSMC. Proteins were separated by IEF in 18-cm-long IPG strips containing a non-linear pH 3–10 gradient followed by SDS-PAGE in vertical 9%–16% gradient gels. Proteins were detected by silver staining

Table 1 Proteins identified by mass spectrometry. Three different classes of proteins were sequenced by mass spectrometry (*Chaperones and redox enzymes*, *Cytoskeleton components*, and *Glucose metabolism enzymes*). Four proteins could not be grouped into a homogeneous class (*Others*). Each protein was identified according to the Mascott database (*Score* −10*Log [*P*], where *P* is the probability that the observed match is a random event). Protein scores greater than 80 are significant ($P<0.05$)

Protein name	ID	Score
Chaperones and redox enzymes		
Hsp60 (60-kDa heat-shock protein, mitochondrial precursor)	P63038	230
PDIA3 (protein disulfide isomerase A3 precursor)	P30101	331
Reticulocalbin 1 precursor	Q15293	151
PRDX4 (peroxiredoxin 4)	O08807	259
PRDX3 (thioredoxin-dependent peroxide reductase, mitochondrial precursor)	P35705	94
Hsp27 (heat-shock protein beta-1, 27 kDa)	P04792	82
Cytoskeleton elements		
Vimentin	P02544	186
Actin alpha	P68032	215
Gamma-actin (actin, cytoplasmic 2)	P63259	117
Tropomyosin4 (tropomyosin alpha 4 chain)	P02561	156
Alpha-tropomyosin (tropomyosin 1 alpha chain)	P58772	210
Cytokeratin 10 (keratin, type I cytoskeletal 10)	P13645	113
Glucose metabolism enzymes		
Pyruvate kinase M1/M2	P14618	140
Pyruvate dehydrogenase E1 component beta subunit, mitochondrial	P11177	94
Alpha enolase	Q9XSJ4	73
ATP synthase D chain, mitochondrial	P13620	80
Others		
Alpha(B)-crystallin (alpha crystallin B chain)	P41316	104
hnRNP H (heterogeneous nuclear ribonucleoprotein H)	O35737	79
Alpha-S1 casein precursor	P02662	337
Prohibitin	P35232	504

important regulatory roles in activated cells and for cell-cycle control (Table 1).

A comparison of the protein profile of VSMC at the onset (quiescent-contractile) and at the terminal stage of the process (activated) reflected a global view of two extreme conditions but did not provide information about the temporal kinetics of the event. Moreover, because the stimulation of growth factor concerned the activation of signal transduction networks characterized by several tyrosine-kinase functions, we wanted to investigate the way that the tyrosine-phosphorylation changed over time in response to FBS administration. With this aim, we analyzed the overall tyrosine-phosphorylation profile of quiescent VSMC (0 time) and of VSMC after 10, 30, and 60 min and 2 days of serum stimulation. The 2D gels were blotted onto nitrocellulose membranes, and phosphorylated spots were detected with an anti-phosphotyrosine-specific monoclonal antibody. Figure 3, which shows the time course of tyrosine-phosphorylation changes, reveals a net decrease of the phosphorylation level within the first 10 min, followed by a slow recovery, with a value close to the starting value after 48 h.

Tyrosine phosphorylation was followed over time for 20 antibody-sensitive spots corresponding to the sequenced proteins (Fig. 4). The phosphorylation of glucose metabolism enzymes greatly decreased at 10 min and remained low for all proteins, except for ATP synthase (Fig. 4a). Chaperones displayed a similar behavior in the first few minutes after stimulus, but PDI and Hsp60 showed a dramatic increase of phosphorylation after 10 and 30 min, respectively, quickly reaching much higher values than those observed initially (Fig. 4b). With regard to cytoskeleton proteins, α-actin and cytokeratin 10 displayed a pattern similar to that of the glucose metabolism enzymes, whereas none of the others varied significantly, at least

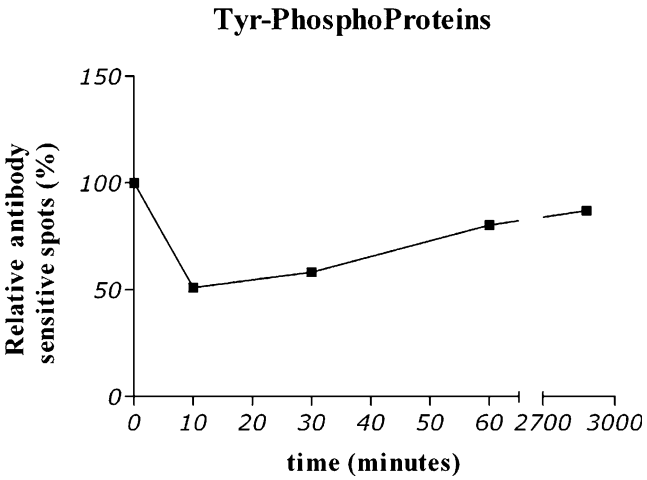

Fig. 3 Time-course experiments. Quiescent VSMC or cells stimulated for 10, 30, or 60 min or 48 h were subjected to 2D-PAGE, the proteins were blotted on nitrocellulose membranes, and the phosphorylated spots were identified by an anti-phosphotyrosine monoclonal antibody. The curve shows the phosphorylation course over time, expressed as the percentage of antibody-sensitive spots relative to time zero

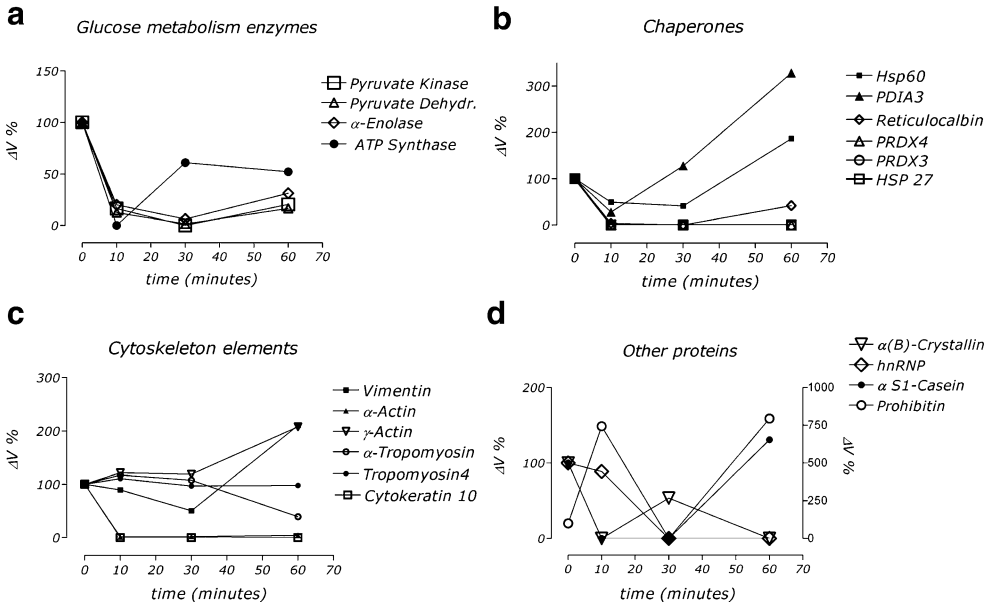

Fig. 4 Tyrosine phosphorylation relative to 20 sequenced proteins. Sequenced proteins were grouped into four classes: glucose metabolism enzymes (**a**), chaperones (**b**), cytoskeleton elements (**c**), and proteins that were not classifiable into a homogeneous category (**d**). The level of phosphorylation is represented as volume percentage (*ΔV%*) of the stained spots. Volume percentage in **d** is represented by two separate scales because of the elevated levels of prohibitin

during the first 30 min of stimulation (Fig. 4c). The remaining proteins displayed non-homogeneous modulation (Fig. 4d).

The time-course data offer a global view of the activation profile concerning the sequenced proteins but do not provide information relating the role of the various factors present in the serum. Moreover, as is apparent from the data presented so far, the most important changes take place during the first 10 min after stimulation, with a general trend subsequently to return to the initial values of phosphorylation within 48 h from the beginning of the process. For all these reasons, we compared the phosphorylation profiles of VSMC stimulated for 10 min with serum or a single growth factor, IGF-1 or PDGF-BB. Remarkable differences were observed (Fig. 5a–d, Table 2). Changes in the phosphorylation patterns were greater after PDGF-BB than after IGF-1 or serum stimulation. Moreover, PDGF-BB seemed to have a principal role in increasing tyrosine-

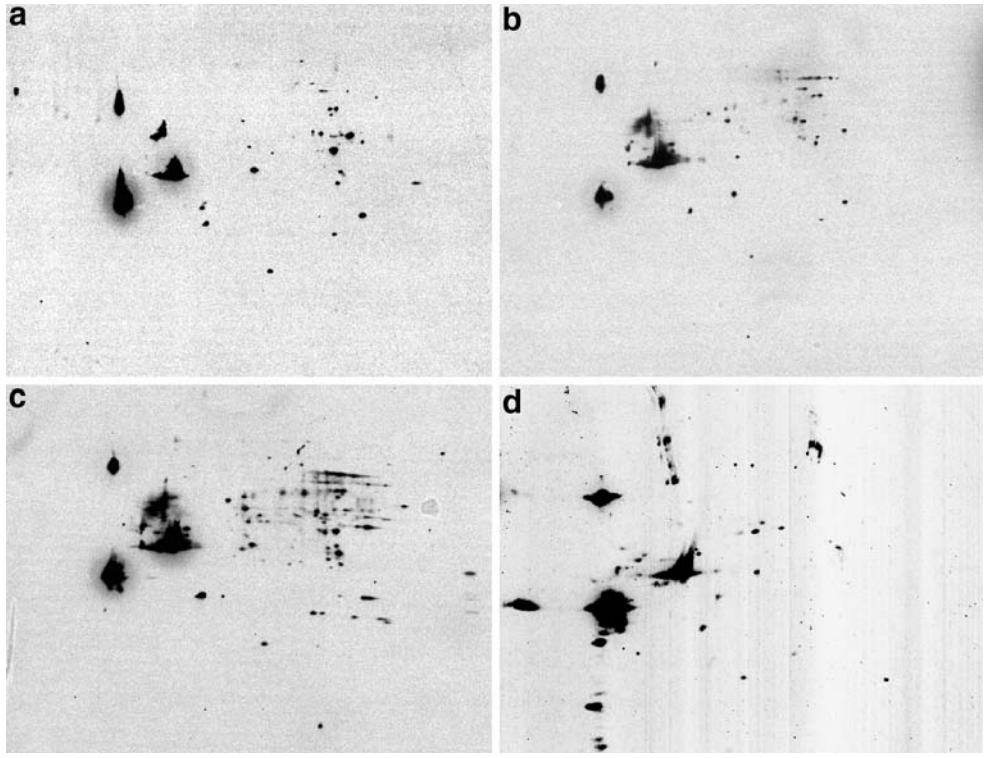

Fig. 5 Tyrosine phosphoproteomes obtained from 2D-PAGE blotted onto nitrocellulose membrane and probed with a specific phosphotyrosine monoclonal antibody. Phosphorylation profiles of quiescent-contractile VSMC (**a**) and after 10 min of stimulation with IGF-1 (**b**), PDGF-BB (**c**), or FBS (**d**)

Table 2 Differentially phosphorylated spots after a 10-min stimulation of quiescent-contractile VSMC with a single growth factor or with serum

	IGF	PDGF	FBS
Up-regulated spots	6	29	10
Down-regulated spots	10	5	15

phosphorylation (85% of modified spots), whereas IGF-1 and serum treatments were characterized by significant dephosphorylation (62% and 60% of modified spots in IGF-1 and FBS, respectively).

Histograms in Fig. 6 reveal the differences in phosphorylation intensity attributable to FBS, IGF-I, or PDGF-BB stimulation for 10 minutes. Tyrosine-phosphorylation changes displayed similar responses for the glucose metabolism enzymes, except for ATP synthase whose phosphorylation did not change after single growth factor stimulation (Fig. 6a). As far as the cytoskeleton components are concerned, different behavior after serum or single growth factor administration was observed (Fig. 6b). Finally, chaperones displayed even more remarkable different responses to serum with respect to single growth factors. Most of them, although reducing their phosphorylation level after 10 min of serum treatment, did not change

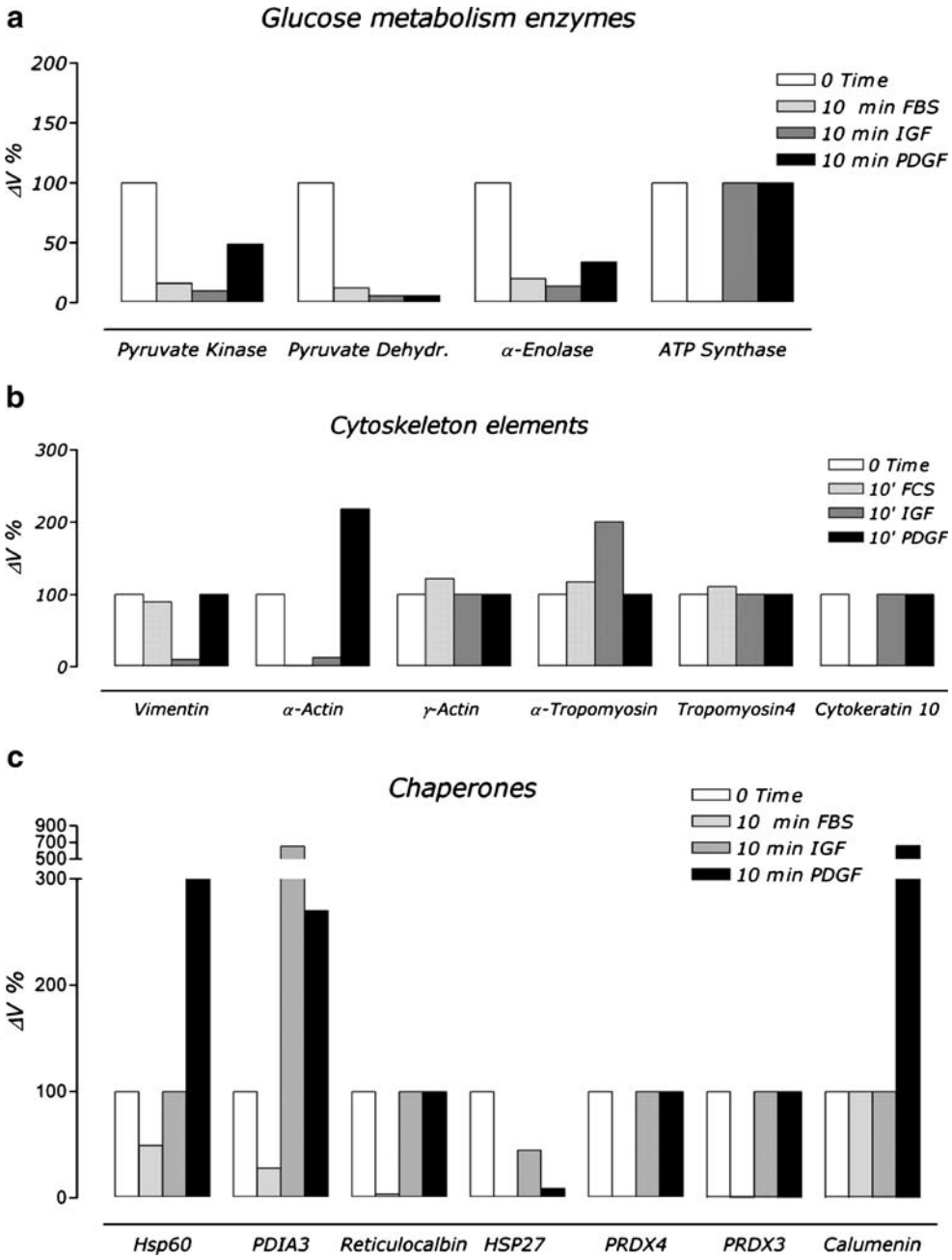

Fig. 6 Comparative analysis of proteins differentially phosphorylated after 10 min by IGF-1, PDGF-BB, or FBS stimulation. The histograms report the tyrosine phosphorylation values expressed as spot volume percentage (*white bars* phosphorylation level of quiescent VSMC at time 0 in reference to which all other values are normalized). Proteins are separated into three homogeneous classes: glucose metabolism enzymes (**a**), cytoskeleton components (**b**), and chaperones (**c**)

or increase their phosphorylation level after single growth factor activation (Fig. 6c).

Discussion

The switching of the VSMC phenotye has a great general relevance for human health, as it is associated with several vascular diseases. The distinction between synthetic and contractile phenotypes proposed by Chamley-Campbell et al. (1979) has been employed for decades and has been useful in planning experiments and inspiring new studies. However, we now realize that such a distinction represents an oversimplification incapable of capturing the complex and dynamic aspects of VSMC phenotype modulation (Owens et al. 2004). Here, we approach this old topic with a novel strategy by investigating, at the protein level, the early changes that prime the signaling cascades leading to the acquisition of a new phenotype.

With this aim, we have analyzed contractile-quiescent and 48-h serum-activated VSMC by 2D-PAGE and have identified some of the differentially expressed proteins. In order to improve our understanding of the cellular pathways involved in the activation process, we have explored the phosphorylation pattern in VSMC during the activation process and have recorded over time the tyrosine-phosphorylation changes for 20 sequenced proteins (from time 0 to 48 h).

Briefly, we have documented an initial general decrease of the tyrosine-phosphorylation level within the first few minutes after stimulation, with a subsequent recovery after 48 h to levels close to those at the start. Thus, in the early stages of the activation course, important and significant events occur favoring the activity of tyrosine phosphatases. This is in accordance with a recent study, suggesting the pivotal importance of phosphatases, such as SHP-2, in directing VSMC toward a specific phenotype (Hayashi et al. 2004). Although descriptive, the data regarding phosphorylation/de-phosphorylation are of interest as they offer a global view of the early response, suggesting a possible role of phosphatases in priming the activation process. This is a novel aspect that deserves to be investigated more extensively.

The phosphorylation kinetics observed during the time-course analysis provide evidence for a homogeneous trend among the different classes of proteins, although the kinetics are specific for each protein. The most significant results concern the chaperones, particularly Hsp60 and PDI whose phosphorylation rate rapidly increases, reaching impressive values much higher than those seen initially. For the glucose metabolism enzymes (with the exception of ATP synthase), there is a slow, yet partial, recovery toward their initial values. As far as cytoskeleton proteins are concerned, changes in tyrosine phosphorylation do not appear to be remarkable, especially at the earliest time points. An important exception is α-actin whose phosphorylation level decreases to 0. This is not surprising as this protein is one of the principal markers of the contractile VSMC (Roy et al. 2001); its expression drops considerably during the activation process as confirmed by our fluorescence microscopy observations. At present, we cannot make any conclusion regarding the degree to which the decrease in phosphorylation signal is attributable to actual de-phosphorylation or to a reduction in protein concentration.

Because 10 min appears to be critical for the triggering the complexity of the activation process following serum administration, we have focused on this time point in order to understand the role of single growth factors. To this purpose, VSMC were treated for 10 min with IGF-1 or PDGF-BB, the phosphorylation profiles were analyzed, and the results compared with those obtained following serum treatment. Of note, chaperones and redox-related enzymes show the most significant differences depending on the treatment. In particular, serum does not seem to be so effective as the single factors for the induction of tyrosine-phosphorylation. For example, Hsp60 and calumenin are phosphorylated following PDGF-BB stimulation, but not after IGF-1 or serum stimulation, whereas PDI is up-phosphorylated after both IGF-1 and PDGF-BB, but serum causes its de-phosphorylation. As far as Hsp27 is concerned, both single growth factors induced a decrease in phosphorylation, but to a smaller extent than serum. From these data, we can conclude that each serum component, depending on its concentration, might control cellular metabolic pathways differently. In other words, as the observed differences in the effects demonstrate, activation is a highly complex process in which each factor has a distinctive and particular role.

Hsp60 has been well demonstrated as being involved in cardiovascular diseases (Snoeckx et al. 2001; Pockley 2002). Barazi et al. (2002) have suggested a role for surface-expressed Hsp60 in mediating the activation of α3β1 integrin by modulating its conformation. Our data, which provide evidence for a post-translational modification of Hsp60 as a result of growth factor stimulation, support the findings of Barazi et al. (2002) and suggest a possible role for Hsp60 in VSMC migration.

Moreover, the data concerning PDI presented herein are in agreement with those of Patton et al. (1995) who have reported the up-regulation of PDI following hyperplastic stimuli, such PDGF and 10% serum. PDI is commonly located in the endoplasmic reticulum, but, like Hsp60, it is also secreted at low levels from a variety of cell types and has been found on the surface of cells (for a review, see Wilkinson and Gilbert 2004). Interestingly, PDI is present

on the surface of rat aortic VSMC in an active reduced conformation and, in this location, might catalyze disulfide interchange in thrombospondin 1 (TSP 1). In this way, PDI might regulate the interaction between TSP 1 and PDGF, playing a role in PDGF targeting to its receptors on VSMC (Hogg et al. 1997).

Hsp27 is reported to have an actin-capping activity that seems to be required for actin polymerization and efficient motility induction, since limiting the length of the growing branches would contribute to generating efficient propulsive forces (Pichon et al. 2004).

Briefly, our results support the concept that chaperones in general, and stress-related proteins in particular, have crucial roles in the first stages of activation process and are presumably connected with cytoskeleton remodeling and cell migration.

In conclusion, the most remarkable feature that occurs during the early stages of VSMC activation, irrespective of growth factor stimulation, is the recruitment of chaperones, i.e., molecules devoted to the maquillage and recycling of previously made proteins, some of them being calcium-regulated and the majority operating on cytoskeleton elements and being related to cell motility. Our study raises a series of issues concerning modulators of cell remodeling and also provides interesting clues regarding the various molecules involved in the early events of cell activation. In our opinion, each single factor that we have identified is worth being investigated more extensively; indeed, we intend to utilize gene knock-down technology to improve the characterization of the function of the factors identified during the process of activation. Our goal is the discovery of switches triggering the early events of VSMC remodeling in order to design new therapeutic strategies for the prevention and treatment of cardiovascular diseases.

Acknowledgments We thank Dr. Dietmar Waidelich and Dr. Dietrich Merkel of Applied Biosystems for their collaboration and kind hospitality at their laboratories in Darmstadt (Germany). We are also grateful to Manuella Walker for helpful reading of the manuscript.

References

Barazi HO, Zhou L, Templeton NS, Krutzsch HC, Roberts DD (2002) Identification of heat shock protein 60 as a molecular mediator of $\alpha 3\beta 1$ integrin activation. Cancer Res 62:1541–1548

Baserga R, Rubin R (1993) Cell cycle and growth control. Crit Rev Eukaryot Gene Expr 3:47–61

Bayes-Genis A, Conover CA, Schwartz RS (2000) The insulin-like growth factor axis: a review of atherosclerosis and restenosis. Circ Res 86:125–130

Candiano G, Bruschi M, Musante L, Cantucci L, Ghiggeri G, Carnemolla B, Orecchia P, Zardi L, Righetti PG (2004) Blue silver: a very sensitive colloidal Coomassie G-250 staining for proteome analysis. Electrophoresis 25:1327–1333

Cercek B, Sharifi B, Barath P, Bailey L, Forrester JS (1991) Growth factors in pathogenesis of coronary arterial restenosis. Am J Cardiol 68:24C–33C

Chamley-Campbell J, Campbell GR, Ross R (1979) The smooth muscle cell in culture. Physiol Rev 59:1–6

Christen T, Bochaton-Piallat ML, Neuville P, Renzen S, Redard M, Eys G van, Gabbiani G (1999) Cultured porcine coronary artery smooth muscle cells: a new model with advanced differentiation. Circ Res 85:99–107

Clemmons DR (1985) Exposure to platelet-derived growth factor modulates the porcine aortic smooth muscle cell response to somatomedin-C. Endocrinology 117:77–83

Delafontaine P, Bernstein KE, Alexander RW (1991) Insulin-like growth factor I gene expression in vascular cells. Hypertension 17:693–699

Delafontaine P, Song Y-H, Li Y (2004) Expression, regulation, and function of IGF-1, IGF-1R, and IGF-1 binding proteins in blood vessels. Arterioscler Thromb Vasc Biol 24:435–444

Dupont A, Corseaux D, Dekeyzer O, Drobecq H, Guihot A-L, Susen S, Vincentelli A, Amouye P, Jude B, Pinet F (2005) The proteome and secretome of human arterial smooth muscle cells. Proteomics 5:585–596

Görg A, Postel W, Günther S (1988) The current state of two-dimensional electrophoresis with immobilized pH gradients. Electrophoresis 9:531–546

Hayashi K, Shibata K, Morita T, Iwasaki K, Watanabe M, Sobue K (2004) Insulin receptor substrate-1/SHP-2 interaction, a phenotype-dependent switching machinery of insulin-like growth factor-I signaling in vascular smooth muscle cells. J Biol Chem 279:40807–40818

Heldin CH, Westermarck B (1990) Platelet derived growth factor: mechanism of action and possible in vivo function. Cell Regul 1:555–566

Hochstrasser DF, Patchornik A, Merril CR (1988) Development of polyacrylamide gels that improve the separation of proteins and their detection by silver staining. Anal Biochem 173:412–423

Hogg PJ, Hotchkiss KA, Jimenez BM, Stathakis P, Chesterman CN (1997) Interaction of platelet-derived growth factor with thrombospondin 1. Biochem J 326:709–716

Kamide K, Hori MT, Zhu JH, Takagawa Y, Barrett JD, Eggena P, Tuck ML (2000) Insulin and insulin-like growth factor-I promotes angiotensinogen production and growth in vascular smooth muscle cells. J Hypertens 18:1051–1056

Kaplan-Albuquerque N, Bogaert YE, Van Putten V, Weiser-Evans MC, Nemenoff RA (2005) Patterns of gene expression differentially regulated by platelet-derived growth factor and hypertrophic stimuli in vascular smooth muscle cells: markers for phenotypic modulation and response to injury. J Biol Chem 280:19966–19976

McGregor E, Kempster L, Wait R, Welson SY, Gosling M, Dunn MJ, Powel JT (2001) Identification and mapping of human saphenous vein medial smooth muscle proteins by two-dimensional polyacrylamide gel electrophoresis. Proteomics 11:1405–1414

Owens GK, Kumar MS, Wamhoff BR (2004) Molecular regulation of vascular smooth muscle cell differentiation in development and disease. Physiol Rev 84:767–801

Patton WF, Erdjument-Bromage H, Marks AR, Tempst P (1995) Components of protein synthesis and folding machinery are induced in vascular smooth muscle cells by hypertrophic and hyperplastic agents. J Biol Chem 270:21404–21410

Pichon S, Bryckaert M, Berrou B (2004) Control of actin dynamics by p38 MAP kinase-Hsp27 distribution in the lamellipodium of smooth muscle cells. J Cell Sci 117:2569–2577

Pockley AG (2002) Heat shock proteins, inflammation, and cardiovascular disease. Circulation 105:1012–1017

Ross R (1993) The pathogenesis of atherosclerosis: a perspective for the 1990s. N Engl J Med 362:801–809

Roy S-G, Nozaki Y, Phan SH (2001) Regulation of alpha-smooth muscle actin gene expression in myofibroblast differentiation from rat lung fibroblasts. Int J Biochem Cell Biol 33:723–734

Rubini M, Werner H, Gandini E, Roberts CT, Leroith D, Baserga R (1994) Plateled-derived growth factor increases the activity of the promoter of the insulin-like growth factor-1 (IGF-1) receptor gene. Exp Cell Res 221:374–379

Shevchenko A, Wilm M, Vorm O, Mann M (1996) Mass spectrometric sequencing of proteins from silver-stained polyacrylamide gels. Anal Chem 68:850–858

Snoeckx LH, Cornelussen RN, Van Nieuwenhoven FA, Reneman RS, Van Der Vusse GJ (2001) Heat shock proteins and cardiovascular pathophysiology. Physiol Rev 81:1461–1497

Thyberg J, Hedin U, Sjölund M, Palmberg L, Bottger BA (1990) Regulation of differentiated properties and proliferation of arterial smooth muscle cells. Arteriosclerosis 10:966–990

Wilkinson B, Gilbert HF (2004) Protein disulfide isomerase. Biochim Biophys Acta 1699:35–44